RSC Advances

PAPER

View Article Online
View Journal | View Issue

Cite this: *RSC Adv.*, 2019, **9**, 22523

Electrocatalytic reduction of trace nitrobenzene using a graphene-oxide@polymerized-manganese-porphyrin composite†

Huanhuan Li, Can Huang, Yingying Li, Weijun Yang * and Fan Liu

A core–shell structure electrocatalyst for trace nitrobenzene reduction was prepared with Mn(II)[5,10,15,20-tetra(4-aminophenyl)porphyrin] (MnTAPP) and graphene oxide (GO) as raw materials. Firstly, MnTAPP and GO were combined together by covalent bonds, and then the supported MnTAPP was coupled together through *p*-dibromobenzene, a conjugated bridging agent, to obtain a more stable graphene-oxide@polymerized-manganese-porphyrin composite (GMPP@AMP). The structure and morphology of the GMPP@AMP were characterized by FT-IR, Raman spectroscopy, SEM and TEM. The GMPP@AMP modified glassy carbon electrode (GMPP@AMP/GCE) was prepared and the electrochemical activity of GMPP@AMP towards nitrobenzene reduction was evaluated by cyclic voltammetry (CV). The results showed that GMPP@AMP/GCE had a more positive reduction potential than MnTAPP/GCE and GO/GCE, and the reduction current responded more sensitively. Electrocatalytic reduction currents of nitrobenzene were found to be linearly related to concentration over the range 0.04 to 0.24 mM using a differential pulse voltammogram (DPV) method. Nitrobenzene is easily compatible with polymerized MnTAPP which has rich nitrogen-containing functional groups and porous structure, and the highly conductive GO combined with the polymerized MnTAPP having excellent electron transfer ability. This produced a significant synergistic catalytic effect during the electrocatalytic reaction of trace nitrobenzene. The novel composite has good application prospects in electrochemical detection of trace nitrobenzene compounds in the environment.

Received 18th April 2019
Accepted 10th July 2019

DOI: 10.1039/c9ra02932j

rsc.li/rsc-advances

Introduction

Nitrobenzene compounds are important chemical raw materials and have been widely used in medicine, pesticides, industrial dyes, and chemical production.[1–4] Because of their own toxicity and hard-to-degrade nature, nitrobenzene compounds have caused great harm to organisms and the environment. Nitrobenzene compounds are also widely used in the military field.[5,6] However, nitrobenzene compounds are slightly soluble in water, so they are difficult to detect.[7] Therefore, the question of how to quickly and efficiently detect trace nitrobenzene compounds has attracted more and more attention from researchers.

At present, various methods have been studied for the detection of trace nitrobenzene compounds, such as liquid chromatography,[8] spectrophotometry,[9] chemiluminescence,[10] surface-enhanced Raman scattering,[11] immunoassay sensing[12] and electrochemical methods.[13] Among them, electrochemical methods have attracted extensive attention due to their advantages such as high efficiency, high sensitivity, simple operation, and low cost.[14,15] In the electrochemical detection method, the selection of the electrode is particularly important. The sensitivity of the bare electrode to the detection object is not enough. Therefore, in order to make the electrode more sensitive, some materials are used to modify the electrode generally. Porphyrin has a large π-conjugated aromatic ring system, which not only has strong affinity for aromatic compounds, but also has excellent electron transfer properties and catalytic redox properties, so they have been applied to the detection of nitroaromatic compounds by researchers.[16] Porous conjugated metalloporphyrins are a new type of catalyst material with better and more stable catalytic properties than metalloporphyrins.[17–19] Graphene oxide is a new type of two-dimensional carbon nanomaterial with excellent charge transfer properties, a large specific surface area and abundant functional groups that are easily modified.[20,21] Therefore, in this paper, a core–shell structure electrocatalyst was synthesized by porous conjugated metalloporphyrins and graphene oxide, with excellent performance in the electrocatalytic reduction of trace nitrobenzene.

Experimental

Materials and instruments

All of the chemical compounds were purchased from Aladdin Reagent Co. Ltd, China, and were all analytical grade without

College of Chemistry and Chemical Engineering, Hunan University, Changsha 410082, China. E-mail: wjyang@hnu.edu.cn

† Electronic supplementary information (ESI) available. See DOI: 10.1039/c9ra02932j

special treatment unless otherwise mentioned. The preparation of MnTAPP is based on previous papers published by our group.[22] GO was prepared from graphite flakes according to the Hummers' method.[23] Distilled deionized water with a resistivity of 18.0 MΩ cm was used in the experiments.

The FT-IR spectra were obtained on a WQF-410 FT-IR spectrometer (Ruili, China) in the range of 4000–400 cm^{-1}. The Raman spectra were carried out on a Labram-010 Laser Raman spectrometer (Horiba, France). The scanning electron microscopy (SEM) image was collected on a Hitachi S-4800 scanning electron microscope (Hitachi, Japan). The transmission electron micrograph (TEM) was carried on a JEM-3010 TEM instrument (JEOL, Japan). The electrochemical measurements were performed by using a CHI 660 electrochemical working station (Chenhua, China).

Synthesis of acyl chloride graphene oxide (GO-COCl)

GO (30 mg) was refluxed in $SOCl_2$ (20 mL) and DMF (1 mL) at 70 °C for 24 h under nitrogen atmosphere to make the carboxyl form the corresponding acyl chlorides. After the reaction, the excess $SOCl_2$ was removed by distillation. Finally, the filter cake was washed with deionized water 4 times and the filter cake was dried under vacuum to obtain GO-COCl.

Synthesis of GO–MnTAPP

GO-COCl (50 mg) and MnTAPP (50 mg) were dissolved in DMF (20 mL) and refluxed at 135 °C for 72 h under nitrogen atmosphere in presence of 1 mL triethylamine (Et_3N). After completion of the reaction, the mixture was cooled to room temperature, and then poured into 300 mL anhydrous ether to precipitate the product. The product was sufficiently isolated by filtration. The solid was washed with CH_2Cl_2 five times, and thin layer chromatography was used to check the filtrate to ensure the absence of MnTAPP in the final washing. Finally, Et_3N was removed by washing with deionized water, and the resulting product was dried under vacuum to obtain GO–MnTAPP.

Synthesis of GMPP@AMP

GO–MnTAPP (100 mg), *p*-dibromobenzene (60 mg), CuI (19 mg), K_2CO_3 (200 mg) and *N*,*N*-dimethylglycine (20 mg) were put into a flask under anaerobic atmosphere. Then 10 mL 1,4-dioxane was added and heated to reflux. After the reaction was completed, the reaction system was cooled to room temperature and then filtered and washed with absolute ethanol, acetone and chloroform, respectively, until the filtrate was colorless. The resulting solid product was dried under vacuum. The synthesis of GMP@AMP is shown in Scheme 1.

Preparation of modified electrodes

1 mg of GO, MnTAPP, GMPP@AMP was dispersed into 1 mL anhydrous ethanol separately, and then 6.5 μL Nafion solution was added, followed by ultrasonic dispersion for 2 h to obtain a well dispersed suspension. 5 μL of the suspension was dispensed on the pre-treated glassy carbon electrode (GCE), and modified electrodes such as GO/GCE, MnTAPP/GCE, GMPP@AMP/GCE were constructed. Then the electrode was dried naturally and used for the determination of nitrobenzene (Scheme 2).

Electrochemical measurements

Electrochemical detections such as Cyclic Voltammetry (CV) and Differential Pulse Voltammetry (DPV) were performed on a CHI 660 electrochemical workstation. In order to eliminate the influence of dissolved oxygen, high-purity N_2 was passed through the solution for 3–5 minutes before the experiment. Electrochemical detection uses a three-electrode system: a modified glassy carbon electrode (GCE) prepared as a working electrode, a carbon black electrode as an auxiliary electrode, and Ag/AgCl as a reference electrode.

Results and discussion

Characterization of GMPP@AMP

The chemical structures of GO–MnTAPP and GMPP@AMP have been confirmed by FT-IR spectra shown in Fig. 1a. The peak at 1720 cm^{-1} in GO which is attributed to the stretching mode of carboxylic moieties (C=O) nearly disappeared in the GO–MnTAPP hybrid and a new peak appeared at 1630 cm^{-1} (–CO–NH–).[24] The stretching band of the amide C–N peak appears stretching band of the amide C–N peak appears at 1270 cm^{-1}. These results clearly indicate the formation of a covalent amide linkage in the GO–MnTAPP hybrid. The polymer showed a characteristic absorption peak of the pyrrole ring at 1073 cm^{-1}, and a characteristic peak of Mn–N at 1008 cm^{-1}, which was similar to MnTAPP and GO–MnTAPP, indicating that the manganese coordinated ion in the polymer is still tightly bound with the porphyrin ring. Due to the coupling of *p*-dibromobenzene, the absorption peak of $-NH_2$ in GMPP@AMP was greatly weakened at 3340 cm^{-1}, and the characteristic *para*-substitution peak of benzene ring at 798 cm^{-1} was significantly enhanced.

Raman spectroscopy is a powerful instrument used to determine significant structural changes. Therefore, Raman measurements were carried out on GO–MnTAPP and GMPP@AMP. From Fig. 1b we can see that the intensity of the D and G peaks of GMPP@AMP has changed. The intensity ratio (I_D/I_G) is related to the crystallinity of the material, the larger the I_D/I_G, the lower the crystallinity of the material. Compared with GO–MnTAPP, the I_D/I_G of GMPP@AMP increased from 0.99 to 1.13, indicating that the crystallinity of the composite was reduced, and the coupling reaction of GO–MnTAPP was also demonstrated.

From the scanning electron microscopy (Fig. 1c), we can clearly see that metalloporphyrin polymer loaded on the surfaces of the graphene oxide, and part of the polymer are stacked together, indicating that some distortion might occurred when the GO–MnTAPP coupled with *p*-dibromobenzene, which causes some polymer surfaces interpenetrate each other instead of simple planar growth. The surface of the composite is rough and porous, which is a characteristic feature of the porphyrin conjugated

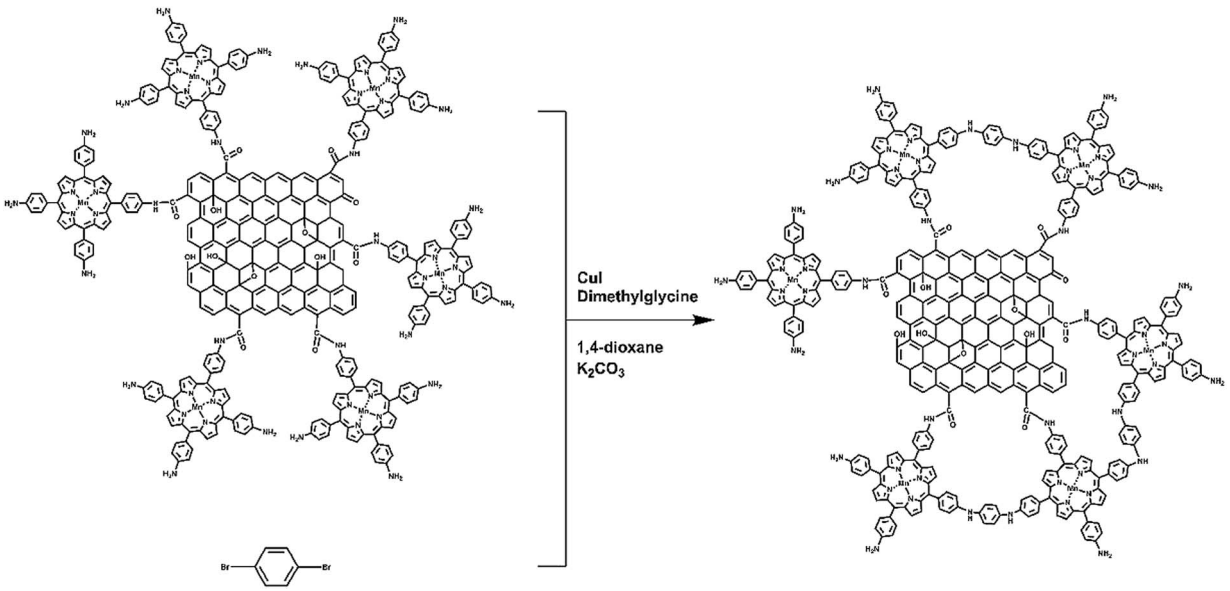

Scheme 1 Synthesis of GMP@AMP.

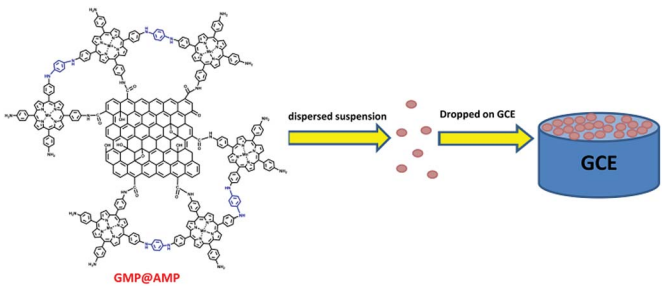

Scheme 2 Preparation of GMPP@AMP/GCE.

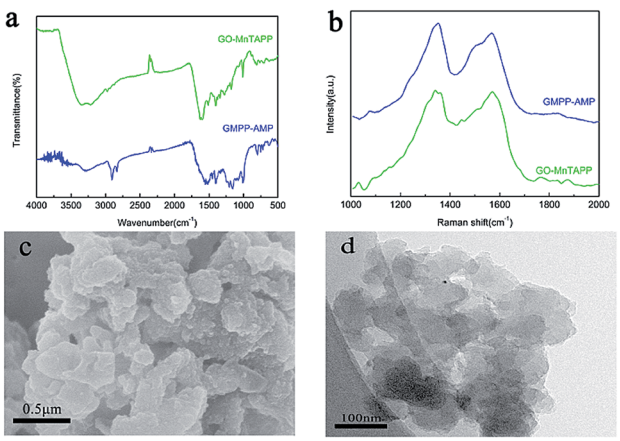

Fig. 1 (a) FT-IR spectra and (b) Raman spectra of GO–MnTAPP and GMPP@AMP; (c) SEM and (d) TEM of GMPP@AMP.

polymer.[17,18] Transmission electron microscopy (Fig. 1d) also proved that the metalloporphyrin polymer stacked each other.

Electrochemical studies

Electrochemical response of different supporting electrolytes to nitrobenzene. In order to compare the electrocatalytic activity of different supporting electrolytes on nitrobenzene, we tested different supporting electrolytes under the same conditions. Fig. 2a shows the CV curves in 0.5 M PBS (pH = 7), 0.5 M NaOH and 0.5 M NaCl solutions containing 0.1 mM nitrobenzene on GMPP@AMP/GCE. It is clear that the electroreduction peak of NaCl solution was sharper and showed a higher catalytic current than that of PBS or NaOH solution. For the reductive peak at −0.75 V, the currents were −92.64, −83.45 and −78.21 μA for NaCl, PBS (pH = 7) and NaOH solution respectively.

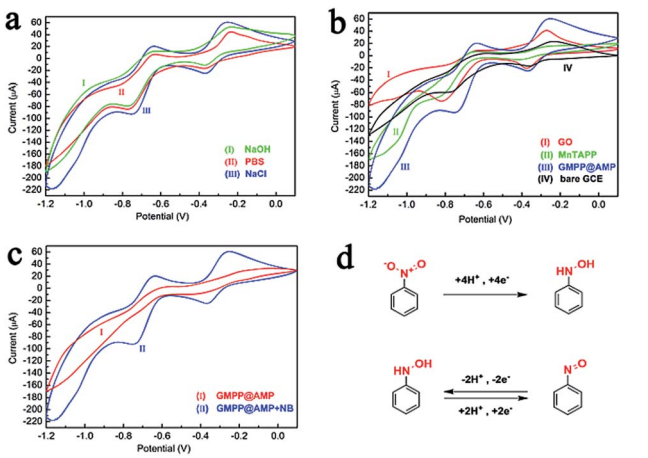

Fig. 2 (a) Cyclic voltammograms of PBS (pH = 7) (I), NaOH (II), NaCl (III) solution containing 0.1 mM nitrobenzene on GMPP@AMP/GCE; (b) cyclic voltammograms of GO/GCE (I), MnTAPP/GCE (II), GMPP@AMP/GCE (III) and bare GCE (IV) in 0.5 M NaCl solution containing 0.1 mM nitrobenzene; (c) cyclic voltammograms of GMPP@AMP/GCE in 0.5 M NaCl solution without (I) and with 0.1 mM nitrobenzene (II); (d) the possible electrochemical mechanism of nitrobenzene.

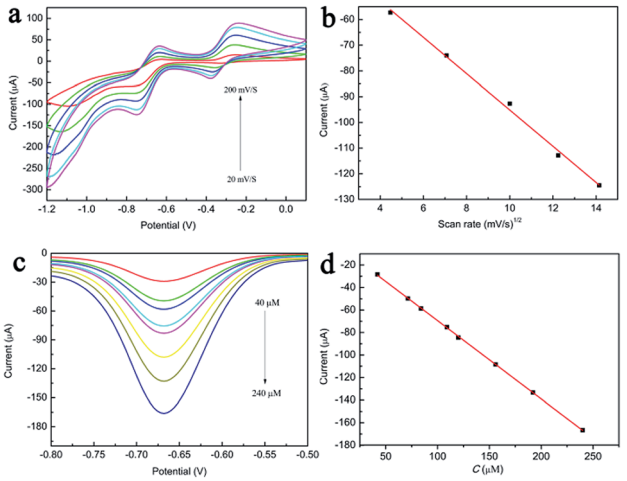

Fig. 3 (a) Cyclic voltammograms of GMPP@AMP/GCE in 0.5 M NaCl solution containing 0.1 mM nitrobenzene at different scan rates (mV s^{-1}): 20, 50, 100, 150, 200; (b) the linear relationship between reduction peak current of nitrobenzene *vs.* the square root of scan rate; (c) differential pulse voltammograms of GMPP@AMP/GCE in 0.5 M NaCl solution containing 0.1 mM nitrobenzene at different concentration (μM): 42, 71, 84, 120, 156, 192, 240; (d) the linear relationship between the reduction peak current *vs.* the varied concentrations of nitrobenzene.

Electrochemical response of different modified electrodes to nitrobenzene. In order to compare the electrocatalytic activity of different modified electrodes on nitrobenzene, we tested different modified electrodes under the same conditions. Fig. 2b shows the CV curves of GO/GCE, MnTAPP/GCE and GMPP@AMP/GCE. The solution is a 0.5 M NaCl solution containing 0.1 mM nitrobenzene. The scan rate is 100 mV s^{-1}, and the initial potential 0.1 V, the high potential 0.1 V, the low potential −1.2 V. N_2 must be introduced for 3–5 minutes before all experiments to eliminate the effect of O_2. From the figure, we can see that MnTAPP/GCE has no obvious electrochemical response to nitrobenzene. This is because the porphyrin of MnTAPP has poor conductivity and its electron transfer resistance is large (Fig. 4a), which hinders the transfer of electrons at the electrode interface, which results in the reduction peak of nitrobenzene in the CV curve is not obvious. However, the electrode modified with GO and GMPP@AMP showed obvious reduction peaks.

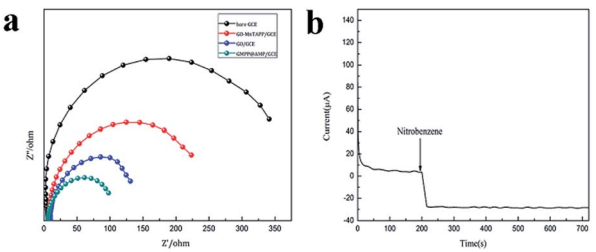

Fig. 4 (a) The Nyquist plots of GMPP@AMP samples in 0.5 M NaCl solution containing 0.1 mM nitrobenzene and (b) current response curve.

The reduction potential of GMPP@AMP/GCE appeared at −0.75 V while that of GO/GCE appeared at −0.8 V, and the reduction potential was shifted by 50 mV compared with GO/GCE. The reduction current of GMPP@AMP/GCE for electrocatalytic reduction of nitrobenzene has more excellent reduction peak current response than other modified electrodes. We analyzed the reasons for the following aspects: firstly, because of the well-developed micro–mesopores on the surface of the MnTAPP polymer, the contact area between the polymer and nitrobenzene is increased. Secondly, there is a strong mutual affinity between nitrobenzene and MnTAPP, making nitrobenzene easy to aggregate and react on the modified electrode. Thirdly, the π–π conjugated macrocycles of porphyrins have good electron mobility and are easily delocalized. Through the charge conduction of the graphene substrate, the manganese ion in the center of the porphyrin ring is further activated, thereby enhancing its electrocatalytic properties. Such factors make the GMPP@AMP/GCE have excellent electrocatalytic properties.

When the GMPP@AMP/GCE is applied to the electrocatalytic reduction of trace nitrobenzene, in comparison with unmodified GCE (Fig. 2b), GMPP@AMP/GCE has shown significantly improved capacitance current indicating good conductivity of the as-prepared microstructures. In the absence of nitrobenzene, no noteworthy peak was observed at GMPP@AMP/GCE. However, highly enhanced peaks were observed in presence of 0.1 mM nitrobenzene (Fig. 2c). The response peak for the reduction of nitrobenzene to phenylhydroxylamine appeared at −0.75 V in the first scanning segment, which was similar to the reported literature.[25,26] The interconversion of nitrosobenzene and phenylhydroxylamine occurred during the reduction of nitrobenzene, resulting in the appearance of a new reduction peak at −0.37 V and a new oxidation peak at −0.25 V in the second scanning segment. These two peaks are also a pair of redox peaks. The specific process is shown in Fig. 2d.

Impedance test

In order to investigate the difference in electron transfer rates of several electrodes, we conducted Electrochemical Impedance Testing (EIS) on these electrodes (Fig. 4a). As can be seen from Fig. 4a, GMPP@AMP/GCE has the smallest electron transfer resistance. The reason for this may be that graphene oxide has poorer conductivity than graphene, and the combination with metal porphyrin polymer can improve its conductivity. The macrocyclic electron delocalization of metal porphyrin polymer has a strong affinity with nitrobenzene, which minimizes the electron transfer resistance at the electrode interface. It can be seen from Fig. 4a that the electron transfer resistance of GMPP@AMP/GCE is smaller than that of GO/GCE, which indicates that the Faraday current of GMPP@AMP/GCE is also larger than that of GO/GCE. That is to say, both the capacitive current and Faraday current of GMPP@AMP/GCE are larger than that of GO/GCE. Therefore, GMPP@AMP/GCE has good electrocatalytic performance.

Current response test

In order to obtain the electrochemical performance parameters of the sensor, under the optimal conditions, the current response test is performed. The tested working potential is −0.75 V, and the

background solution is 0.5 M NaCl solution (pH = 7). After the background current is stabilized, 20 μL of a 0.1 mM nitrobenzene solution was added dropwise thereto. It can be seen from Fig. 4b that when nitrobenzene is added to the electrolyte solution, the current response time of GMPP@AMP/GCE is 120 s, which is a short response time.

Effect of the scan rate

The effect of scan rate on the electrocatalytic behaviour of GMPP@AMP/GCE was investigated at different scan rates ranging from 20 to 200 mV s^{-1} in 0.5 M NaCl solution containing 0.1 mM nitrobenzene. It can be seen from Fig. 3a that both the reduction peak current and the oxidation peak current of nitrobenzene were increased as the scan rate increases.

Taking the reduction peak of nitrobenzene at −0.75 V as an example, it can be seen from Fig. 3b that there is a good linear relationship between the reduction peak current intensity and $v^{1/2}$ (R^2 = 0.995), and with the increase of scanning rate, the response current of nitrobenzene reduction peak also increases. This shows that the redox process of nitrobenzene catalyzed by GMPP@AMP/GCE is mainly controlled by diffusion.

Effect of the nitrobenzene concentration

We investigated the electrochemical response of GMPP@AMP/GCE to different concentrations of nitrobenzene by differential pulse voltammetry (DPV). Fig. 3c is a differential pulse voltammograms of nitrobenzene on GMPP@AMP/GCE at different concentrations. As it can be seen in the figure, with increasing nitrobenzene concentration, the reduction peak current of nitrobenzene by GMPP@AMP/GCE also increased. Fig. 3d shows that there is a good linear relationship between the reduction peak current intensity and concentration of the nitrobenzene (R^2 = 0.996). The linear equation is $I/\mu A = -0.609c/(\mu M) - 18.928$. The sensitivity is $0.609A/(\text{mol L}^{-1})$, and the linear range is 34–246 μM. The DPV test was carried out 10 times with a 0.5 M NaCl standard solution containing no nitrobenzene. The current value at −0.75 V is shown in Table S1,† and the standard deviation was 0.04925, thereby calculating the detection limit of 0.243 μM (S/N = 3). Compared with previous reports on the detection of nitrobenzene by electrochemical sensors (Table 1),[25–30] GMPP@AMP/GCE has a wider linear range and lower detection limit, which is mainly attributed to the good affinity between the complex and nitrobenzene, and the synergistic catalysis of graphene oxide makes it easier for nitrobenzene to aggregate on the electrode surface and generate electrochemical reduction.

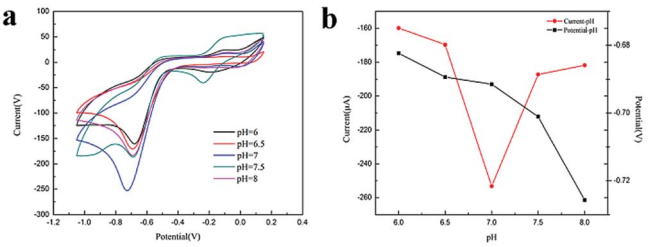

Fig. 5 (a) pH in the range of 6–8. CV curve of GMPP@AMP/GCE in 0.5 M NaCl solution containing 0.1 mM nitrobenzene; (b) peak current and peak voltage *versus* pH.

Effect of pH

pH value is an important parameter in electrochemical detection, which can affect the electrochemical response sensitivity of electrochemical sensors to detectors. It has been found from a large number of literatures that the optimum range of pH response for nitroaromatic compounds is between 6 and 8.[31–38] In order to investigate the effect of pH value on the sensitivity of GMPP@AMP/GCE for the detection of trace nitrobenzene, cyclic voltammetry (CV) was performed for the buffer of sodium hydrogen phosphate/sodium dihydrogen phosphate (PBS) in the range of pH 6–8 (Fig. 5). It was found that the reduction peak current of nitrobenzene increased initially with the increase of pH, reached its maximum at 7, and then decreased with the increase of pH. The results show that the electrochemical behavior of nitrobenzene depends on pH and the concentration of hydrogen ion will affect the reaction rate of the electrode. In addition, the reduction peak potential shifted negatively with the increase of pH, indicating that H^+ was involved in the electrochemical reaction of nitrobenzene, which further verified the reaction mechanism mentioned above. Therefore, in all subsequent experiments, pH = 7 was selected for further study. The cyclic voltammetry of GMPP@AMP/GCE in 0.5 M NaCl solution containing 0.1 mM nitrobenzene was studied. The pH value at the beginning of the experiment was 6.8 and at the end of the experiment was 7.4. The pH value of the experiment remained between 6 and 8, which was closer to the real situation of nitrobenzene wastewater than other solution.

Table 1 Comparison of analytical performance with some modified electrodes for electrochemical determination of NB

Electrode	pH	Linear range (μM)	LOD (M)	Reference
GRGO-Ni-TPP/GCE	PBS (pH = 7)	0.5–878	0.14×10^{-6}	25
OMC/DDAB/GCE	PBS (pH = 7)	25–2900	0.1×10^{-5}	26
γ-Al_2O_3/GCE	PBS (pH = 7)	0.5–145.5	0.15×10^{-6}	27
CMF-RGO	PBS (pH = 7)	0.2–927.7	0.88×10^{-7}	28
NiCuk/GCE	PBS (pH = 7)	100–20 000	0.4×10^{-4}	29
MWCNTs/GCE	PBS (pH = 9)	0.08–32.5	0.24×10^{-7}	30
GMPP@AMP/GCE	NaCl (pH = 7)	34–246	0.243×10^{-6}	This work

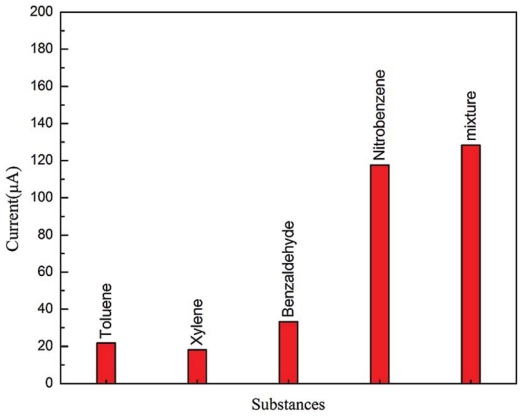

Fig. 6 Peak current of DPV curve in toluene, xylene and benzaldehyde. (* Mixture refers to the mixture of toluene, xylene, benzaldehyde and nitrobenzene with a concentration of 0.1 mM.)

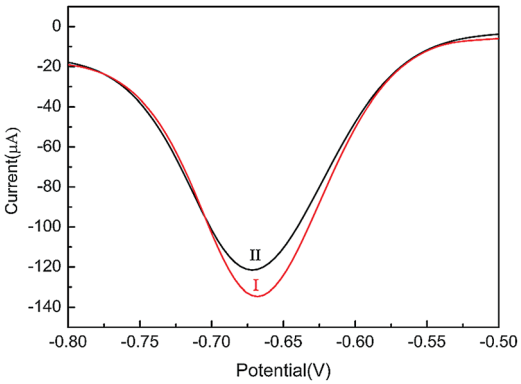

Fig. 7 Differential pulse voltammograms of GMPP@AMP/GCE in 0.5 M NaCl solution containing 0.1 mM nitrobenzene: first time (I); after 20 days (II).

Sample reproducibility and selectivity

In order to measure the reproducibility of GMPP@AMP, we used the DPV method to continuously scan 10 times in 0.5 M NaCl solution, and GMPP@AMP/GCE as the working electrode, and measured the peak current value at −0.75 V, as shown in Table S2 (ESI).† Its relative standard deviation is 3.13% (<5%), indicating that it has good reproducibility.

We selected aromatic compounds such as toluene, *p*-xylene and benzaldehyde which are rich in pion electrons for electrochemical experiments. As can be seen from Fig. 6, the corresponding response current is obvious in the electrolyte solution containing nitrobenzene, while the response current of toluene, *p*-xylene and benzaldehyde is very weak, which indicates that GMPP@AMP/GCE electrode has good selectivity for the electrochemical detection of nitrobenzene. This may be due to the fact that nitrobenzene is more easily affinity with porphyrin rings in the structure of GMPP@AMP/GCE, even though toluene, xylene, benzaldehyde and nitrobenzene all contain benzene rings and are easily enriched on the surface of GMPP@AMP/GC. And another reason is that it is difficult to reduce toluene, xylene and benzaldehyde in this electrolyte solution system, so their reaction current is not obvious. Therefore, GMPP@AMP/GCE has better selectivity for the reaction of nitrobenzene.

Real sample analysis

Nitrobenzene was not detected in tap water, so different concentrations of nitrobenzene were added to tap water (0.5 M NaCl solution was added to tap water, and the ratio of tap water to 0.5 m NaCl solution was 1 : 5). After 60 s concentration, DPV of these water samples was tested with GMPP@AMP/GCE, and three parallel tests were carried out for each water sample. The concentration of nitrobenzene in each sample was obtained by standard curve (Fig. 3d). The experimental results are shown in Table S3.† According to Table S3,† the recovery rate of GMPP@AMP/GCE for tap water detection is 94.65–98.6%. This indicates that GMPP@AMP has the potential to be applied to the detection of nitrobenzene in actual water samples.

Stability of GMPP@AMP/GCE

We also explored the stability of GMPP@AMP/GCE. We stored the tested electrode in a refrigerator at 4 °C and tested it again after 20 days. The current intensity was still above 90%, indicating that GMPP@AMP/GCE has good stability (Fig. 7).

Conclusions

Using acyl chloride graphene oxide as the main reactant, the tetraaminophenyl manganese porphyrins were immobilized on the surface of graphene oxide and were coupled together by *p*-dibromobenzene, thus a composite of GO encapsulated by the polymerized MnTAPP (GMPP@AMP) was obtained. The GMPP@AMP was modified on a glassy carbon electrode to realize the electrocatalytic reduction of nitrobenzene. Electrochemical detection shows that GMPP@AMP has a good electrocatalytic activity for trace nitrobenzene. The trace nitrobenzene is easy to be affined with MnTAPP which is rich in nitrogen-containing functional groups, and the abundant micro–mesopore structures in polymeric metalloporphyrins also tend to adsorb the trace nitrobenzene. The highly conductive GO combined with the polymerized MnTAPP with excellent electron transfer ability produced a significant synergistic catalytic effect in the electrocatalytic reaction of nitrobenzene, making this novel composite have good application prospects in electrochemical detection of trace nitrobenzene in the environment.

Conflicts of interest

There are no conflicts to declare.

Acknowledgements

The authors are thankful for financial support from the National Natural Science Foundation of China (Grant no. 21576074). The authors are also grateful for the financial support of Hunan University.

References

1 D. Zhang, X. Zeng, Z. Yu, G. Sheng and J. Fu, Determination of nitrobenzenes and nitrochlorobenzenes in water samples using dispersive liquid-liquid microextraction and gas chromatography-mass spectrometry, *Anal. Methods*, 2011, **3**, 2254–2260.

2 K. S. Ju and R. E. Parales, Nitroaromatic compounds, from synthesis to biodegradation, *Microbiol. Mol. Biol. Rev.*, 2010, **74**, 250–272.

3 J. Zhang, Y. Zhang and X. Quan, Bio-electrochemical enhancement of anaerobic reduction of nitrobenzene and its effects on microbial community, *Biochem. Eng. J.*, 2015, **94**, 85–91.

4 Y. P. Li, H. B. Cao, C. M. Liu and Y. Zhang, Electrochemical reduction of nitrobenzene at carbon nanotube electrode, *J. Hazard. Mater.*, 2007, **148**, 158–163.

5 P. Rameshkumar and R. Ramaraj, Electroanalysis of nitrobenzene derivatives and nitrite ions using silver nanoparticles deposited silica spheres modified electrode, *J. Electroanal. Chem.*, 2014, **731**, 72–77.

6 K. Cizek, C. Prior, C. Thammakhet, M. Galik, K. Linker, R. Tsui, A. Cagan, J. Wake, J. La Belle and J. Wang, Integrated explosive preconcentrator and electrochemical detection system for 2, 4, 6-trinitrotoluene (TNT) vapor, *Anal. Chim. Acta*, 2010, **661**, 117–121.

7 N. Sahiner, S. Yildiz and H. Al-Lohedan, The resourcefulness of p(4-VP) cryogels as template for in situ nanoparticle preparation of various metals and their use in H2 production, nitro compound reduction and dye degradation, *Appl. Catal., B*, 2015, **166**, 145–154.

8 J. Bečanová, Z. Friedl and Z. Šimek, Identification and determination of trinitrotoluenes and their degradation products using liquid chromatography–electrospray ionization mass spectrometry, *Int. J. Mass Spectrom.*, 2010, **291**, 133–139.

9 T. M. Green, P. T. Charles and G. P. Anderson, Detection of 2, 4, 6-trinitrotoluene in seawater using a reversed-displacement immunosensor, *Anal. Biochem.*, 2002, **310**, 36–41.

10 R. Freeman and I. Willner, NAD+/NADH-sensitive quantum dots: applications to probe NAD+-dependent enzymes and to sense the RDX explosive, *Nano Lett.*, 2008, **9**, 322–326.

11 M. Liu and W. Chen, Graphene nanosheets-supported Ag nanoparticles for ultrasensitive detection of TNT by surface-enhanced Raman spectroscopy, *Biosens. Bioelectron.*, 2013, **46**, 68–73.

12 J. C. Sanchez, A. G. DiPasquale, A. L. Rheingold and W. C. Trogler, Synthesis, luminescence properties, and explosives sensing with 1, 1-tetraphenylsilole-and 1, 1-silafluorene-vinylene polymers, *Chem. Mater.*, 2007, **19**, 6459–6470.

13 R. Wen, H. X. Zhang, C. J. Yan, H. J. Yan, G. B. Pan and L. J. Wan, TNT adsorption on Au (111): electrochemistry and adlayer structure, *Chem. Commun.*, 2008, 1877–1879.

14 B. Qi, F. Lin, J. Bai, L. Liu and L. Guo, An ordered mesoporous carbon/didodecyldimethy lammonium bromide composite and its application in the electro-catalytic reduction of nitrobenzene, *Mater. Lett.*, 2008, **62**, 3670–3672.

15 H. X. Zhang, A. M. Cao, J. S. Hu, L. J. Wan and S. T. Lee, Electrochemical sensor for detecting ultratrace nitroaromatic compounds using mesoporous SiO2-modified electrode, *Anal. Chem.*, 2006, **78**, 1967–1971.

16 Y. Salinas, A. Agostini, É. Pérez-Esteve, R. Martínez-Máñez, F. Sancenón, M. D. Marcos, J. Soto, A. M. Costero, S. Gil and M. Parra, Fluorogenic detection of Tetryl and TNT explosives using nanoscopic-capped mesoporous hybrid materials, *J. Mater. Chem. A*, 2013, **1**, 3561–3564.

17 Y. Li, B. Sun and W. Yang, Synthesis of conjugated Mn porphyrin polymers with p-phenylenediamine building blocks and efficient aerobic catalytic oxidation of alcohols, *Appl. Catal., A*, 2016, **515**, 164–169.

18 Z. Tan, J. Zhu and W. Yang, Conjugated copper (II) porphyrin polymer and N-hydroxyphthalimide as effective catalysts for selective oxidation of cyclohexylbenzene, *Catal. Commun.*, 2017, **94**, 60–64.

19 Y. Li, L. Wang, Y. Gao, W. Yang, Y. Li and C. Guo, Porous metalloporphyrinic nanospheres constructed from metal 5, 10, 15, 20-tetraksi (4′-ethynylphenyl) porphyrin for efficient catalytic degradation of organic dyes, *RSC Adv.*, 2018, **8**, 7330–7339; D. Zhang, X. Zeng, Z. Yu, G. Sheng and J. Fu, *Anal. Methods*, 2011, **3**, 2254–2260.

20 D. A. Dikin, S. Stankovich, E. J. Zimney, R. D. Piner, G. H. Dommett, G. Evmenenko, S. T. Nguyen and R. S. Ruoff, Preparation and characterization of graphene oxide paper, *Nature*, 2007, **448**, 457.

21 Y. Zhu, S. Murali, W. Cai, X. Li, J. W. Suk, J. R. Potts and R. S. Ruoff, Graphene and graphene oxide: synthesis, properties, and applications, *Adv. Mater.*, 2010, **22**, 3906–3924.

22 J. Zhu, Z. Tan and W. Yang, Synthesize polymeric manganese porphyrin with CuI/N, N-dimethyl glycine acid catalytic system and high-efficiency aerobic catalytic oxidation of cyclic ketones, *Macromol. Res.*, 2017, **25**, 792–798.

23 W. S. Hummers Jr and R. E. Offeman, Preparation of graphitic oxide, *J. Am. Chem. Soc.*, 1958, **80**, 1339.

24 X. Zhang, Y. Feng, P. Lv, Y. Shen and W. Feng, Enhanced reversible photoswitching of azobenzene-functionalized graphene oxide hybrids, *Langmuir*, 2010, **26**, 18508–18511.

25 S. Kubendhiran, S. Sakthinathan, S. M. Chen, P. Tamizhdurai, K. Shanthi and C. Karuppiah, Green reduction of reduced graphene oxide with nickel tetraphenyl porphyrin nanocomposite modified electrode for enhanced electrochemical determination of environmentally pollutant nitrobenzene, *J. Colloid Interface Sci.*, 2017, **497**, 207–216.

26 B. Qi, F. Lin, J. Bai, L. Liu and L. Guo, An ordered mesoporous carbon/didodecyldimethylammonium bromide composite and its application in the electro-catalytic reduction of nitrobenzene, *Mater. Lett.*, 2008, **62**(21–22), 3670–3672.

27 B. Thirumalraj, S. Palanisamy, S. M. Chen, K. Thangavelu, P. Periakaruppan and X. H. Liu, A simple electrochemical platform for detection of nitrobenzene in water samples using an alumina polished glassy carbon electrode, *J. Colloid Interface Sci.*, 2016, **475**, 154–160.

28 P. Balasubramanian, T. S. T. Balamurugan, S. M. Chen, T. W. Chen, T. W. Tseng and B. S. Lou, A simple architecture of cellulose microfiber/reduced graphene oxide nanocomposite for the electrochemical determination of nitrobenzene in sewage water, *Cellulose*, 2018, **25**(4), 2381–2391.

29 Z. Yan, Z. Xu, W. Zhang, S. Zhao and Y. Xu, A novel electrochemical nitrobenzene sensor based on NiCu alloy electrode, *Int. J. Electrochem. Sci.*, 2012, **7**, 2938–2946.

30 A. R. Fakhari and H. Ahmar, A new method based on headspace adsorptive accumulation using a carboxylated multi-walled carbon nanotubes modified electrode: application for trace determination of nitrobenzene and nitrotoluene in water and wastewater, *Anal. Methods*, 2011, **3**(11), 2593–2598.

31 Y. Sang, Y. Cui, Z. Li, W. Ye, H. Li, X. Zhao and P. Guo, Electrochemical reaction of nitrobenzene and its derivatives on glassy carbon electrode modified with $MnFe_2O_4$ colloid nanocrystal assemblies, *Sens. Actuators, B*, 2016, **234**, 46–52.

32 Y. Li, Y. Yang, Y. Sun, X. Gao, L. Chen, W. Zhang and S. Chen, A novel reaction system for cogeneration of chemicals and electric energy by electrochemical reduction of nitrobenzene with iron, *Int. J. Electrochem. Sci.*, 2016, **11**, 3502–3511.

33 M. C. F. Oliveira, Study of the hypophosphite effect on the electrochemical reduction of nitrobenzene on Ni, *Electrochim. Acta*, 2003, **48**, 1829–1835.

34 C. Liu, A. Y. Zhang, D. N. Pei and H. Q. Yu, Efficient electrochemical reduction of nitrobenzene by defect-engineered TiO2–x single crystals, *Environ. Sci. Technol.*, 2016, **50**, 5234–5242.

35 Z. Xue, H. Lian, C. Hu, Y. Feng, F. Zhang, X. Liu and X. Lu, Electrochemical reduction and detection of nitrobenzene based on porphyrin composite-modified glassy carbon electrode, *Aust. J. Chem.*, 2014, **67**, 796–804.

36 S. Kubendhiran, S. Sakthinathan, S. M. Chen, P. Tamizhdurai, K. Shanthi and C. Karuppiah, Green reduction of reduced graphene oxide with nickel tetraphenyl porphyrin nanocomposite modified electrode for enhanced electrochemical determination of environmentally pollutant nitrobenzene, *J. Colloid Interface Sci.*, 2017, **497**, 207–216.

37 R. Karthik, M. Govindasamy, S. M. Chen, V. Mani, R. Umamaheswari and T. S. T. Balamurugan, Electrochemical study of nitrobenzene reduction using Potentiostatic preparation of nephrolepis leaf like silver microstructure, *Int. J. Electrochem. Sci.*, 2016, **11**, 6164–6172.

38 N. Gowthaman, B. Sinduja and S. A. John, Tuning the composition of gold–silver bimetallic nanoparticles for the electrochemical reduction of hydrogen peroxide and nitrobenzene, *RSC Adv.*, 2016, **6**, 63433–63444.